Applied Physics Letters

Topological insulators for the generation of electron beams

Cite as: Appl. Phys. Lett. **113**, 233504 (2018); https://doi.org/10.1063/1.5052415
Submitted: 17 August 2018 . Accepted: 27 October 2018 . Published Online: 07 December 2018

Y. Tian, G. Gu, P. Johnson, T. Rao, T. Tsang, and E. Wang

Topological insulators for the generation of electron beams

Y. Tian,[a] G. Gu, P. Johnson, T. Rao, T. Tsang, and E. Wang
Brookhaven National Laboratory, Upton, New York 11973, USA

(Received 17 August 2018; accepted 27 October 2018; published online 7 December 2018)

Measurements of photo-yields from various topological insulators (TIs) in ultra-high vacuum were made. Marked differences in the photoelectric yield were found between the freshly in-vacuum cleaved and the atmosphere cleaved TI samples. The spectral dependence of their quantum efficiency (QE) was obtained in as-cleaved and cesiated TI samples. Inferred work functions ranging from 5 to 5.5 eV were found in all TI samples before cesiation, and they were lowered by ~0.5 eV after cesiation. At the ultraviolet wavelength of 268 nm, the QE of all samples is $\sim 2 \times 10^{-7}$ before cesiation but improved to 10^{-4}–10^{-3} after cesiation. Knowledge of the QE has practical implication and can serve as a useful guide for the development of a spin-polarized electron source. However, the spin polarized nature of the photo-emitted electron remains yet to be explored. *Published by AIP Publishing.* https://doi.org/10.1063/1.5052415

High quality photocathode development is essential for future electron accelerator facilities.[1,2] For the new colliders under consideration, spin-polarized electron beams with ~10 mA CW current, ~5 nC charge, stable electron beam current, and long lifetime are needed.[3] Currently, the strained GaAs photocathode is the only practical candidate that can provide spin-polarized electrons with high quantum efficiency (QE). The typical photo-yield of GaAs before cesium activation is nearly zero, and after cesium activation, it is generally improved to ~1% at 800 nm where the polarization peaks.[4] However, it typically has a short lifetime due to its extreme sensitivity to residual gas contamination above a vacuum level of $\sim 10^{-12}$ Torr and to the integrity on the thin activation layer of cesium atoms.[5] Here, we investigate photoelectric emission from layered, stoichiometric topological insulator (TI) single crystals Bi_2Se_3, Bi_2Te_3, and $Bi_{1.3}Sb_{0.7}(Te_{1.3}Se_{1.7})$,[6] see Fig. 1, as a potential platform for the generation of spin-polarized electrons.[7–10]

Topological insulators are a new class of materials that are insulating in the bulk but with metallic electron states on the surface.[11] The latter states are topologically protected with spin orthogonal to momentum such that back scattering is not allowed.[12] With long electron mean free paths, photoemission from TI photocathodes can potentially produce electron beams with lower intrinsic emittance and faster temporal response. Therefore, they hold great promise for the development of future spintronic devices including the generation of spin-polarized electrons. Experimentally, photoelectron spin polarizations of ~80% have been measured using angle-resolved photoemission spectroscopy (ARPES)[13] but with extreme ultraviolet (XUV) photons. These results point to the prospect of using TI as the photocathodes to generate polarized electron beams for many applications, including electron accelerators. However, the quantum efficiency of TI has not been reported and techniques to improve it are not yet well established. The work function of typical TI is nearly 5 eV[14,15] requiring deep UV lasers which are scarce and impractical. Here, we explore a conventional surface treatment by depositing a thin layer of cesium to lower the work function of the TI, resulting in a higher photoelectric yield.[16,17]

Our system consists of an ultrahigh vacuum chamber where samples can be cleaved *in situ* at $\sim 10^{-12}$ Torr. A schematic of the optical arrangement for quantum efficiency measurements is shown in Fig. 1(a). All TI samples are grown in-house by the Material science department using the Bridgeman method. A uniform carrier concentration was achieved in an ingot of several centimeters in length and of several millimeters in diameter. The TI samples are attached to the stainless-steel table by a high temperature cured silver epoxy. An aluminum cylindrical stud is then epoxied on the top surfaces of all three TI samples. Two sets of the three different TI samples together with two reference metals (silver and gold) are processed together in any single experiment. One set of TI samples is cleaved in ambient air and then immediately installed in the chamber, while another set of samples is cleaved in-vacuum after the system reaches $\sim 10^{-12}$ Torr vacuum level, see Figs. 1 and 2. Three replications of identical experiments were conducted on three duplicate sets of samples to ensure reproducibility. The TI photocathodes are electrically isolated so that voltage bias can be applied and the photocurrent leaving the TI photocathode measured.

A solarization-resistant UV optical fiber system is used to deliver the UV photons to the surface of the TI photocathodes with an illumination spot of ~1 mm in diameter. A hammer for *in-vacuum* sample cleaving and an optical fiber adaptor for securing a bare optical fiber for sample illumination are attached to a linear mechanical manipulator mounted on a three-axis port-aligner, see Fig. 2(b). The samples are cleaved in vacuum simultaneously exposing a mirror-like cleavage (0001) plane in a dimension of $\sim 10 \times 10$ mm^2, see Figs. 2(b) and 2(c). The smoothness of the cleaved sample can be seen on the AFM image where a tapping scan mode is employed. Other than an ~4 nm crystal dislocation plane was observed in the field of view, the sample appeared smooth, see Fig. 2(d). A height profile along the green line of the AFM image highlights the atomic smoothness and the calculated ~0.4 nm rms roughness of the sample.

[a]Author to whom correspondence should be addressed: yitian@bnl.gov

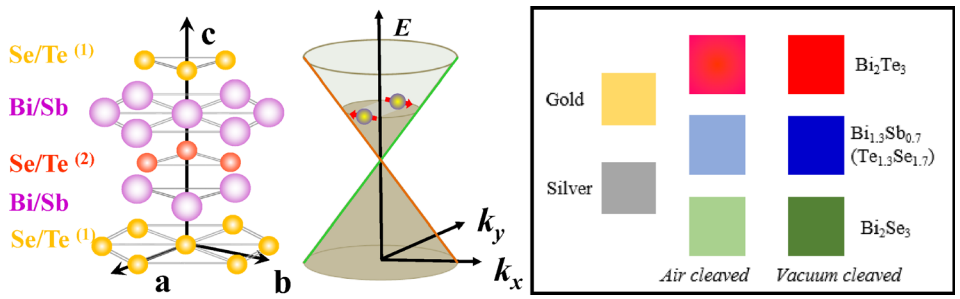

FIG. 1. Left panel: a representative TI sample crystal structure, $Bi_{1.3}Sb_{0.7}(Te_{1.3}Se_{1.7})$; they all share the same rhombohedral crystal structure and space group with five atoms in one-unit cell. Middle panel: a representative TI Dirac dispersion (3-d energy versus momentum plot), E represents the electron energy, k_x and k_y the electron momentum, the yellow balls depict the electrons, and the red arrows represent their spin vectors, which are locked perpendicular to the k_i momentum. Right panel: the layout schematic of two sets of TI samples. One set is air cleaved, and the other set is vacuum cleaved; gold and silver are used as reference metals.

We employ two UV photon sources for sample illumination: (1) For routine QE measurements and monitoring during cesiation, an UV LED operated at the wavelength of 268 nm with an ~16 μW average power delivered to the TI photocathode through an optical fiber is used. (2) For the spectral dependence measurements of QE, a fiber-coupled UV white light (Energetiq, LDLS EQ-99XFC) spectrally selected by a monochromator in a 10-nm bandwidth resulting in 1–20 μW of unpolarized UV photons delivered to the photocathode at normal incidence is used. All optical power is measured prior to making the connection to the in-vacuum UV fiber feedthrough. A negative 20 V bias is applied to the TI and the charge leaving the TI photocathode is measured using an electrometer (Keysight B2987A) on a logarithmic scale. The TI photocathode is activated by application of cesium while monitoring the photocurrent of one sample, Bi_2Te_3 or Bi_2Se_3, with a 268 nm UV LED light until the photo-yield peaks. Based on our previous experience on GaAs, the typical thickness of the multilayer cesium atom deposited on the TI photocathode would be on the nanometer scale.[18] Although the uniformity of cesium coverage among different TI samples was not monitored, the consistency of their photo-yield on various runs with the repositioned cesium source suggested that cesium coverage was largely uniform.

In measurements of the photo-yield employing a continuous wave photon source, the quantum efficiency (QE) is defined as $\frac{\text{measured photocurent (Amp)}}{\text{optical power (Watt)}} \times \text{photon energy (eV)}$. By measuring the emitted photocurrent and incident photon power at a given photon energy, we can then calculate the spectral dependence of the QE. Measurements are done on all TI samples, air cleaved and vacuum cleaved, before and after cesiation. For comparison, a 99.99% purity noble metal gold foil that has also been cesiated at the same time with the TI samples is used as a reference. Typical optical power illuminating the photocathode ranges from μW level to ~100 mW at various spectral wavelengths with different spectral bandwidths, while measured photocurrent ranges from pA to ~100 nA. To ensure that the photoelectrons are space charge free, a current versus voltage (I–V) scan was performed from low to high photocurrent conditions, ~pA, ~nA, and ~100 nA, see Fig. 3. It is evident that at the applied bias voltage of –20 volt, electrons are not space charge-limited. In addition, a linear one-photon photoelectric emission is confirmed before or after cesiation, see the inset of Fig. 3.

The spectral dependence on the QE of Bi_2Se_3, $Bi_{1.3}Sb_{0.7}(Te_{1.3}Se_{1.7})$, and Bi_2Te_3 from 3 eV to 6.2 eV photons is shown in Figs. 4(a), 4(c), and 4(e), respectively, on a semi-log scale plot, highlighting the orders of magnitude change in QE under various conditions. Unlike metals where the work function can be positively determined from the intercept of a square root of the QE versus photon energy ($h\nu$) plot, $\sqrt{QE} \sim (h\nu - \varphi)$,[19,20] where φ is the work function, topological insulators are non-metallic, and their exact work function cannot be clearly extracted from the spectral dependence. Nonetheless, one can qualitatively infer their work functions when electrons cease to emit below a certain photon energy. In Figs. 4(b), 4(d), and 4(f), the QE data near the threshold are plotted on a linear scale to locate the intercept

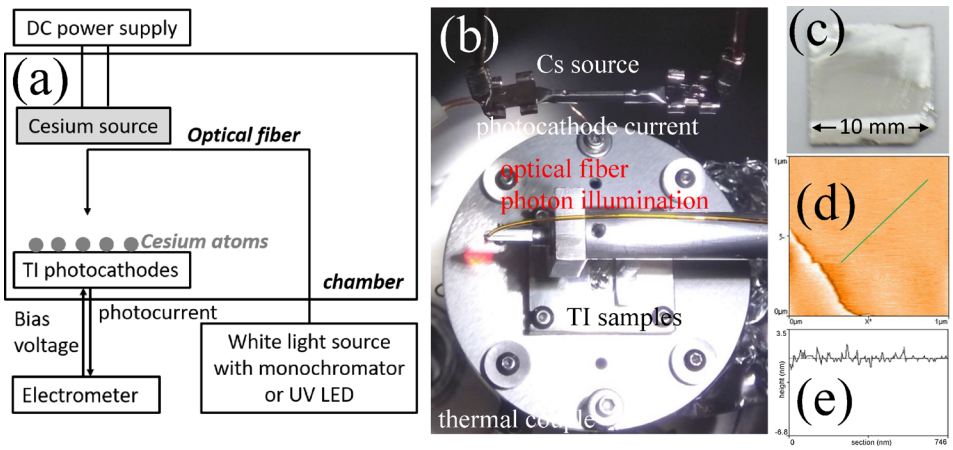

FIG. 2. (a) Schematic of the optical arrangement for quantum efficiency measurements. (b) Details of the *in-vacuum* sample cleaving arrangement and the in-vacuum optical fiber for sample illumination. (c) An optical picture of a cleaved Bi_2Te_3 and (d) its corresponding AFM image, $1 \times 1\ \mu m^2$, highlighting a crystal dislocation plane, otherwise atomic smoothness with a calculated rms roughness of ~0.4 nm depicted by (e) the height profile along the green line of the AFM image.

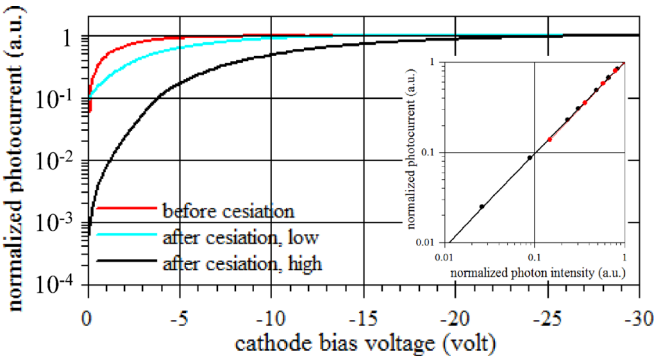

FIG. 3. Photocurrent versus bias voltage (I–V) plot of a TI sample (Bi_2Te_3) at various stages of the experiment, illustrating the space charge free measurements before and after cesiation. Inset: linearity of the electron emission against photon intensity for all cases (same color coding scheme) confirming the 1-photon linear photoemission process. "Low" and "high" correspond to $\sim\mu$W and ~100 mW optical power level, respectively.

and to infer the work functions. The inferred work functions of in-vacuum cleaved Bi_2Se_3, $Bi_{1.3}Sb_{0.7}(Te_{1.3}Se_{1.7})$, and Bi_2Te_3 are all in the range of ~5.5 eV and lowered to 5.12 eV, 4.53 eV, and 4.15 eV, respectively, after cesiation, see Table I. The inferred work functions of the corresponding air-cleaved TI samples are in the range of ~4.8 eV, and they are lowered to 4.47 eV, 4.47 eV, and 4.3 eV, respectively.

The spectral dependence on the photo-yield of TI obeyed the DuBridge theoretical description,[20] with electron yield generally increasing logarithmically with photon energy and saturating at high UV photon energy. However, we note that the QE of all in-vacuum cleaved TI photocathodes before cesiation is generally low $\sim 2 \times 10^{-7}$ at 260 nm, see Table II. In contrast, noble metals are typically in $\sim 10^{-5}$ at the same UV wavelength under identical bias field gradient.[21] Therefore, even if spin polarized electrons were favorably generated on TI photocathodes, the low QE may reduce their importance as a suitable electron source. After cesium deposition, the QE of all TI generally increased by 2 to 3 orders of magnitude to 10^{-4} to 10^{-3}, with larger (smaller) enhancement in the lower (higher) photon energy. In contrast to the in-vacuum cleaved TI photocathodes, air-cleaved samples

TABLE I. Inferred work function (eV) of TI samples before and after cesiation.

Work function (eV)	Bi_2Se_3		$Bi_{1.3}Sb_{0.7}(Te_{1.3}Se_{1.7})$		Bi_2Te_3	
Cesiation	Before	After	Before	After	Before	After
Vacuum cleaved	5.35	5.12	5.56	4.53	5.56	4.15
Air cleaved	4.80	4.47	4.90	4.47	4.70	4.3

collectively have >2 orders of magnitude higher QE than their corresponding vacuum cleaved samples, see Figs. 4(a), 4(c), 4(e), and Table II. However, after cesiation, their QE improvements are substantially less. It is interesting to note that after cesiation, both vacuum-cleaved and air-cleaved TI photocathodes arrived at nearly the same QE $\sim 10^{-4}$, but they are not identical. For comparison, we note that cesium activated GaAs generally have ~1% QE at 800 nm where the polarization peaks. We hypothesise that our photo-yield is not intrinsic to the cesium layer. First, the deposited cesium layers are ~nm multilayer thick much thinner the ~127 nm penetration depth of UV photons. Therefore, photons will illuminate the TI samples and can directly generate photoelectrons. Second, the QE of cesiated Bi_2Te_3 is consistently higher than that of $Bi_{1.3}Sb_{0.7}(Te_{1.3}Se_{1.7})$, which is also consistently higher than that of Bi_2Se_3. This consistent QE behavior was observed on several repeated measurements on the same or different sets of samples done on different days. Conversely, after cesiation, the work function of Bi_2Te_3 (4.15 eV) is lower than that of $Bi_{1.3}Sb_{0.7}(Te_{1.3}Se_{1.7})$ (4.53 eV) and is lower than the work function of Bi_2Se_3 (5.12 eV). Therefore, we concluded that the electron emission is likely not intrinsic to the cesium layers. Otherwise, all TI samples would have the same QE and correspondingly the same reduced work function. However, we note that the definitive confirmation depends on our on-going spin polarization measurements.

Vacuum or air cleaved samples show no appreciable change in photo-yield or spectral characteristics in 10^{-12} Torr ultrahigh vacuum over a long period of time (days and weeks) even when they are illuminated with >10 mW high UV photons generating >10 nA photocurrent; that is, their carrier

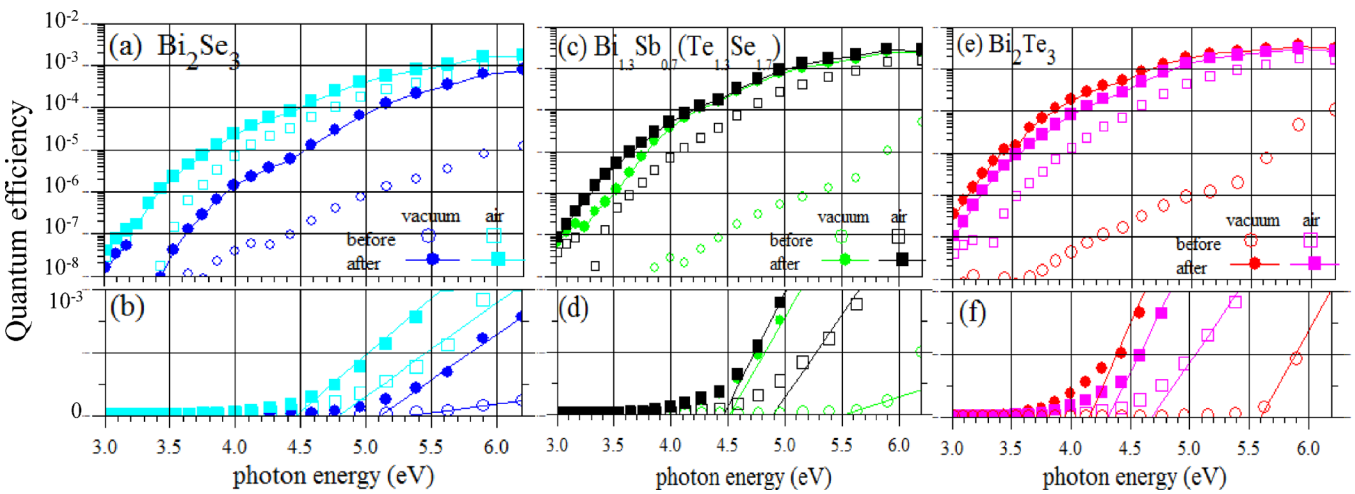

FIG. 4. Spectral dependence on the quantum efficiency of (a) Bi_2Se_3 vacuum-cleaved (blue) and air-cleaved (cyan) before (open circle and box) and after (solid circle and box) cesium deposition on a semi-log scale. (b) QE of Bi_2Se_3 plotted on a linear scale highlighting the inferred work functions, and the lower QE of the vacuum-cleaved before cesiation data (blue open circle) plotted on the same right-hand side linear y-scale but ×10 instead. (c) and (d) Same but for sample $Bi_{1.3}Sb_{0.7}(Te_{1.3}Se_{1.7})$. (e) and (f) Same but for sample Bi_2Te_3.

TABLE II. Quantum efficiency of TI samples before and after cesiation at 268 nm.

QE at 268 nm	Bi_2Se_3		$Bi_{1.3}Sb_{0.7}(Te_{1.3}Se_{1.7})$		Bi_2Te_3		Gold	
Cesiation	Before	After	Before	After	Before	After	Before	After
Vacuum cleaved	2×10^{-7}	1.3×10^{-5}	3.1×10^{-7}	2.8×10^{-4}	3.1×10^{-7}	8.2×10^{-4}	3.1×10^{-5}	2.6×10^{-4}
Air cleaved	5.7×10^{-5}	7.7×10^{-5}	7.4×10^{-5}	3.1×10^{-4}	1.3×10^{-4}	4.8×10^{-4}		

density remains nearly unchanged. In contrast, after cesiation, all samples have small but noticeable photo-yield degradation with time despite sitting in an ultrahigh vacuum environment. This QE degradation worsens and is irreversible with higher UV illumination photon flux accompanied by a slight vacuum loading during illumination, see Fig. 5. Quantitatively, the QE drops ~10–20% in 20 min of continuous UV illumination at ~10 Watt/cm^2. However, QE nearly regained its original value upon re-cesiation of the same samples. We speculate that cesium atoms are being desorbed at higher UV photon flux. Similar behavior has also been observed on cesiated GaAs.[18] A different cesiation procedure may be required to maintain its stability, such as the yo-yo cesiation process[17] routinely used in GaAs or the thermal activation process used in multi-alkali photocathodes.[22]

The large difference in the QE between vacuum-cleaved and air-cleaved TI photocathodes is noteworthy. It is conceivable that because the Fermi level of vacuum-cleaved samples lies only a few tenths of eV above the energy associated with the Dirac point, the relatively low density of states in TI may result in a relatively low surface electron density on the vacuum-cleaved TI samples. Therefore, only a small amount of charge transfer to the vacuum level is possible leading to a lower photoelectron yield. In contrast, the possibly larger electron affinity of air-cleaved samples placed the vacuum level well below the Fermi level, allowing more charge transfer to take place with higher electron density leading to more free electrons available and thus possibly a higher photoelectron yield. Additionally, in the case of air cleaved samples, the adsorbed foreign atoms on the sample surface, such as oxygen, will act as an electron donor giving rise to a higher carrier density on the surface layers. However, typical as-prepared, vacuum cleaved TI samples are suggested to be n-type doped and become further n-type-doped when exposed to atmosphere.[23] The more possible photoelectron contribution from the bulk conduction band could challenge the desired goal of achieving a spin-polarized electron source.

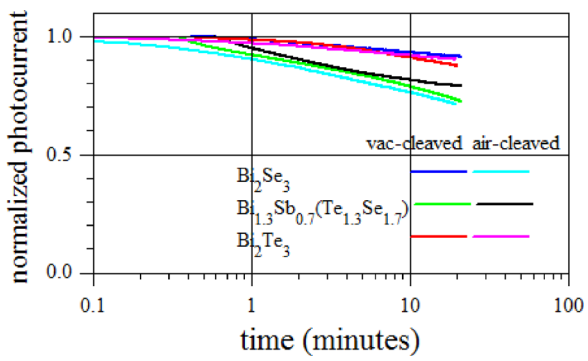

FIG. 5. Stability of cesiated TI photocathodes over time under strong ~10 W/cm^2 UV photon illuminations.

When cesium atoms are deposited on the TI surface, the carrier density can possibly be raised, leading to a lower work function. Our results suggest that both higher carrier density and lowering of the work function may contribute to larger photo-yield on cesiated and air cleaved TI photocathodes, respectively.

We have measured the photoelectric emission on various topological insulators (TIs) in the ultrahigh vacuum condition. Marked differences in the photoelectric yield are found between the freshly in-vacuum cleaved and in-atmosphere cleaved samples. The spectral dependence of their quantum efficiency (QE) is obtained on as-cleaved and cesium-deposited TI samples. Inferred work functions ranging from 5 to 5.5 eV are found on all TI samples before cesiation and reduced by ~0.5 eV after cesiation. Nevertheless, the reduction in the work function alone cannot account for the large change in the photo-yield. Their QE at the ultraviolet wavelength of 268 nm is in the range of $\sim 2 \times 10^{-7}$ before cesiation and improved to 10^{-4} to 10^{-3} after cesiation. The spectral dependence on the QE of as-cleaved and cesiated TI samples has been measured systematically. This work has practical implication for the development of spin polarized electron sources.[9,10]

We emphasise that while the difference in the QE between vacuum-cleaved and air-cleaved TI photocathodes is significant, their QE enhancement after cesiation remains similar. However, the highest ~0.3% QE can be achieved with deep UV photons at ~6 eV on Bi_2Te_3 after cesiation, and this is in sharp contrast to the typical few percent QE achieved on the cesiated GaAs photocathode driven with near-infrared photons. An alternative, photo-yield enhancement technique may need to be explored on TI photocathodes for the efficient generation of spin polarized beams in accelerators. Finally, additional work needs to be done to explicitly confirm the spin polarized nature of the photo-emitted electrons.

This work was supported by the U.S. Department of Energy under Contract No. DE-AC02-98CH10886.

[1]E. C. Aschenauer, M. D. Baker, A. Bazilevsky, K. Boyle, S. Belomestnykh, I. Ben-Zvi, S. Brooks, C. Brutus, T. Burton, S. Fazio *et al.*, e-print arXiv:1409.1633.
[2]D. H. Dowell, I. Bazarov, B. Dunham, K. Harkay, C. Hernandez-Garcia, R. Legg, H. Padmore, T. Rao, J. Smedley, and W. Wan, NIM A **622**, 685 (2010).
[3]E. Wang, International Workshop on Physics with Positrons at Jefferson Lab, AIP Conf. Proc. **1970**, 050008 (2018).
[4]T. Maruyamaa, A. Brachmanna, J. E. Clendenina, T. Desikana, E. L. Garwina, R. E. Kirbya, D.-A. Luha, J. Turnera, and R. Prepost, NIM A **492**, 199 (2002).

[5]C. K. Sinclair, P. A. Adderley, B. M. Dunham, J. C. Hansknecht, P. Hartmann, M. Poelker, J. S. Price, P. M. Rutt, W. J. Schneider, and M. Steigerwald, Phys. Rev. Spec. Top. Accel. Beams **10**, 023501 (2007).
[6]J. Zhao, Z. Yu, Q. Hu, Y. Wang, J. Schneeloch, C. Li, R. Zhong, Y. Wang, Z. Liu, and G. Gu, Phys. Chem. Chem. Phys. **19**, 2207 (2017).
[7]A. V. Subashiev, L. G. Gerchikov, Y. A. Mamaev, Y. P. Yashin, J. S. Roberts, D.-A. Luh, T. Maruyama, and J. E. Clendenin, Appl. Phys. Lett. **86**, 171911 (2005).
[8]Y. A. Mamaev, L. G. Gerchikov, Y. P. Yashin, D. A. Vasiliev, V. V. Kuzmichev, V. M. Ustinov, A. E. Zhukov, V. S. Mikhrin, and A. P. Vasiliev, Appl. Phys. Lett. **93**, 081114 (2008).
[9]X. Jin, A. Mano, F. Ichihashi, N. Yamamoto, and Y. Takeda, Appl. Phys. Express **6**, 015801 (2013).
[10]X. Jin, B. Ozdol, M. Yamamoto, A. Mano, N. Yamamoto, and Y. Takeda, Appl. Phys. Lett. **105**, 203509 (2014).
[11]H. Zhang, C.-X. Liu, X.-L. Qi, X. Dai, Z. Fang, and S.-C. Zhang, Nat. Phys. **5**, 438 (2009).
[12]L. Fu and C. L. Kane, Phys. Rev. B **76**, 045302 (2007).
[13]C. Jozwiak, C.-H. Park, K. Gotlieb, C. Hwang, D.-H. Lee, S. G. Louie, J. D. Denlinger, C. R. Rotundu, R. J. Birgeneau, Z. Hussain, and A. Lanzara, Nat. Phys. **9**, 293 (2013).
[14]D. Haneman, J. Phys. Chem. Solids **11**, 205 (1959).
[15]D. Takane, S. Souma, T. Sato, T. Takahashi, K. Segawa, and Y. Ando, Appl. Phys. Lett. **109**, 091601 (2016).
[16]K. L. Jensena, J. Appl. Phys. **99**, 124905 (2006).
[17]W. Liu, S. Zhang, M. Stutzman, and M. Poelker, Phys. Rev. Accel. Beams **19**, 103402 (2016).
[18]B. Chang, R. Fu, Z. Zong, Y. Qian, Q. Zhan, P. Gao, X. Du, and L. Liu, Proc. SPIE **4796**, 33 (2003).
[19]K. L. Jensen, IEEE Trans. Plasma Sci. **46**, 1881 (2018).
[20]L. A. Dubridge, Phys. Rev. **43**, 727 (1933).
[21]T. Srinivasan-Rao, J. Fischer, and T. Tsang, J. Appl. Phys. **69**, 3291 (1991).
[22]L. Cultrera, C. Gulliford, A. Bartnik, H. Lee, and I. Bazarov, J. Appl. Phys. **121**, 055306 (2017).
[23]M. T. Edmonds, J. T. Hellerstedt, A. Tadich, A. Schenk, K. M. O'Donnell, J. Tosado, N. P. Butch, P. Syers, J. Paglione, and M. S. Fuhrer, J. Phys. Chem. C **118**, 20413 (2014).